JOURNAL OF APPLIED ELECTROCHEMISTRY 19 (1989) 188–194

The influence of mass transport on the deposit morphology and the current efficiency in pulse plating of copper

O. CHÈNE, D. LANDOLT

Laboratoire de Métallurgie Chimique, Département des Matériaux, Ecole Polytechnique Fédérale, CH-1007 Lausanne, Switzerland

Received 19 June 1988

The morphology of copper deposits formed by pulse plating from an acid sulphate electrolyte is investigated. The steady and non-steady state conditions of mass transport are controlled by use of a rotating hemispherical electrode. Below the limiting pulse current density (i_{pl}), granular deposits are observed. Above i_{pl}, regardless of the individual values of the pulse parameters, dendritic deposits are formed. Measured current efficiencies are compared with a theoretical model, which predicts a rapid decrease of the efficiency with the increasing of i_p/i_{pl} for i_p/i_{pl} greater than one, where i_p is the applied pulse current density. For a given set of pulse parameters, the measured current efficiency increases with the deposit thickness due to the increase of the effective surface area. This effect is particularly important for dendritic deposits.

Nomenclature

- A apparent (effective) surface area (cm^2)
- A_0 geometrical surface area (cm^2)
- D diffusion coefficient ($cm^2 s^{-1}$)
- i current density ($A cm^{-2}$)
- i_l limiting current density ($A cm^{-2}$)
- i_p pulse current density ($A cm^{-2}$)
- i_{pl} pulse limiting current density ($A cm^{-2}$)
- i_m average current density in pulse plating ($A cm^{-2}$)
- N_p dimensionless number $N_p = i_p/i_{pl}$
- N_m dimensionless number $N_m = i_m/i_l$
- t_p pulse time (s)
- t'_p relaxation time (s)
- γ duty cycle, $\gamma = t_p/(t_p + t'_p)$
- δ (steady state) diffusion layer thickness (cm)
- δ_p pulsating diffusion layer thickness (cm)
- θ current efficiency
- ν kinematic viscosity ($cm^2 s^{-1}$)
- ω rotation rate ($rad s^{-1}$)

1. Introduction

Theoretical and practical aspects of pulse plating are described in a recent book [1]. One of the most interesting features of using pulsating current (p.c.) instead of direct current (d.c.) is the possibility of influencing deposit morphology by varying the pulse parameters. A number of authors have studied how the choice of these parameters affects deposit morphology [2–6], but our understanding of the many factors which determine the microstructure of electrodeposits is still unsatisfactory. Solution side mass transport [7], nucleation rate [8, 9], adsorption–desorption reactions [7, 8] and recrystallization [7] have been mentioned to play a role. To better understand the relative importance of these and possibly other factors it is necessary to carry out deposition experiments under carefully defined experimental conditions with different metal–electrolyte systems.

The purpose of the present study is the investigation of the influence of solution-side steady state and non-steady state mass transport on the microstructure of copper deposits produced by pulse plating from an acid sulphate electrolyte.

2. Theoretical considerations

In pulse plating steady state and non-steady state mass transport must be taken into consideration [10, 11]. In the present study the steady state mass transport rate is controlled by the use of a rotating hemispherical electrode (RHE). The RHE, compared to the rotating disk electrode (RDE), offers the advantage of having a uniform primary current distribution. On the other hand, the diffusion layer thickness varies slightly in the radial direction [12] but this effect is considered of minor importance here. The average limiting current density on the RHE, calculated by Chin [13], is

$$i_l = 0.474nFc_bD^{2/3}\nu^{-1/6}\omega^{1/2} \quad (1)$$

where c_b is the bulk concentration of the reacting species, D the diffusion coefficient, ν the kinematic viscosity and ω the rotation rate in $rad s^{-1}$. The corresponding value of the mean steady state diffusion layer thickness δ is

$$\delta = 2.11D^{1/3}\nu^{1/6}\omega^{-1/2} \quad (2)$$

Non-steady state mass transport in pulse plating with constant current pulses has been discussed by a

0021-891X/89 $03.00 + .12 © 1989 Chapman and Hall Ltd.

number of authors [10, 14–17] and the functional dependence of the pulse limiting current density on applied pulse parameters has been investigated. The pulse limiting current density, i_{pl}, is the pulse current density at which the surface concentration of reacting species at the cathode for a set pulse time, t_p, and relaxation time, t'_p, reaches zero at the end of the pulse [15]. The semi-empirical expressions 3 and 4, based on Ibl's linear diffusion model, yield i_{pl} values very close (< 3%) to those resulting from more exact numerical calculations [14]. They will be used in the present paper for the characterization of mass transport conditions.

$$i_{pl} = i_l \left[\frac{\delta_p}{\delta}(1 - \gamma) + \gamma \right]^{-1} \tag{3}$$

$$\delta_p = \left[\frac{4}{\pi} D t_p (1 - \gamma) \right]^{1/2} \tag{4}$$

Here δ_p is the pulsating diffusion layer thickness introduced by Ibl [15] and $\gamma = t_p/(t_p + t'_p)$ is the duty cycle.

The (time) average current density i_m in pulse plating is given by Equation 5 where i_p is the pulse current density.

$$i_m = \gamma i_p \tag{5}$$

From the above arguments it follows that mass transport conditions in pulse plating can be characterized by two dimensionless numbers:

$$N_m = i_m/i_l$$

$$N_p = i_p/i_{pl}$$

The value of N_m characterizes steady state, that of N_p non-steady state mass transport conditions. Using Equations 5 and 3 one obtains a relationship between N_p and N_m:

$$\frac{N_p}{N_m} = 1 + \frac{\delta_p}{\delta}\left(\frac{1-\gamma}{\gamma}\right) \tag{6}$$

Since $\gamma \leqslant 1$ it follows that $N_p/N_m \geqslant 1$ in all cases, which sets the limits of the experimental parameter space. If a large range of conditions is to be investigated, a small N_m must be chosen.

Moreover, it has been shown by Cheh [18] that the average deposition rate in pulse plating cannot exceed that corresponding to the d.c. limiting current under otherwise identical conditions, i.e. $\theta_m i_m \leqslant i_l$ where θ_m is the current efficiency for the metal deposition.

3. Experimental details

The cathode is a rotating hemispherical electrode (RHE) of 5 mm radius (1.57 cm^2 working area) produced by cold drawing of a circular copper plate. The hemispherical cap forming the working electrode fits over a copper rod attached to the rotating shaft. The sides are insulated by a piece of silicon tubing tightly fitted over the cap and the copper rod. The tubing is cut precisely to the right length using a specially designed cutter [19]. The described electrode assembly has the advantage of easy interchange of the hemispherical caps which can thus be removed after deposition experiments for weighing and for studying the microstructure.

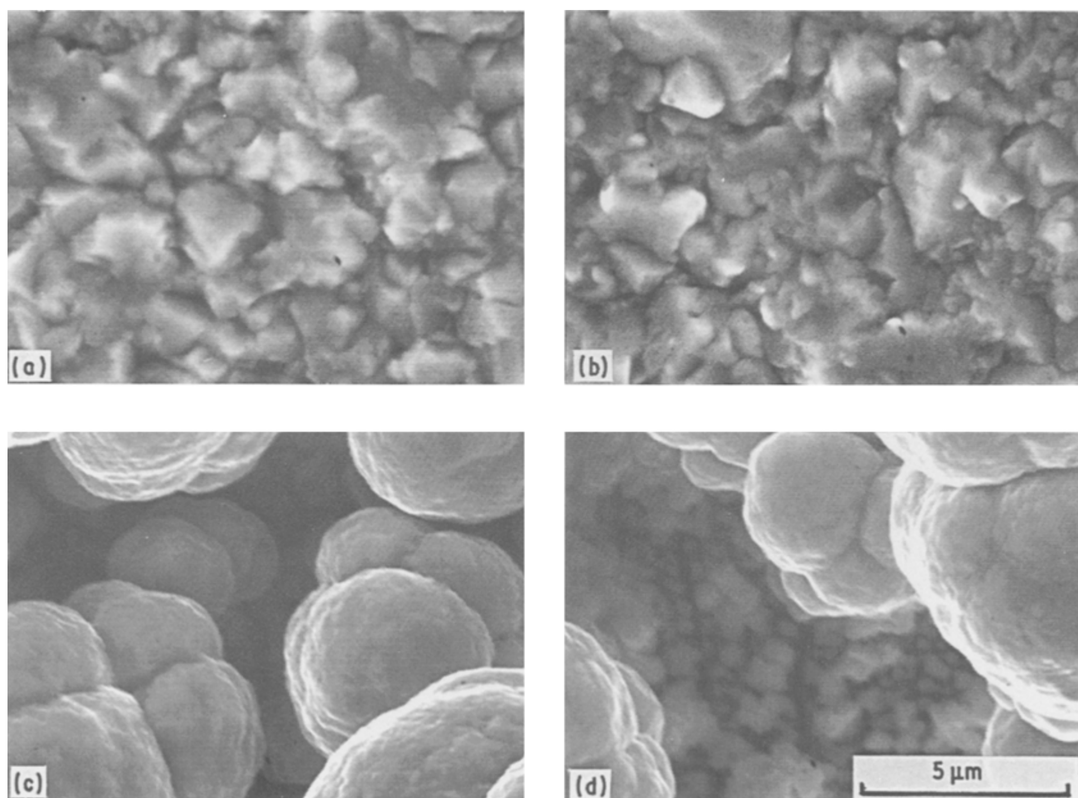

Fig. 1. Deposit morphology observed with direct current at different values of i/i_l: (a) 0.19; (b) 0.8; (c) 1.2; (d) 2.

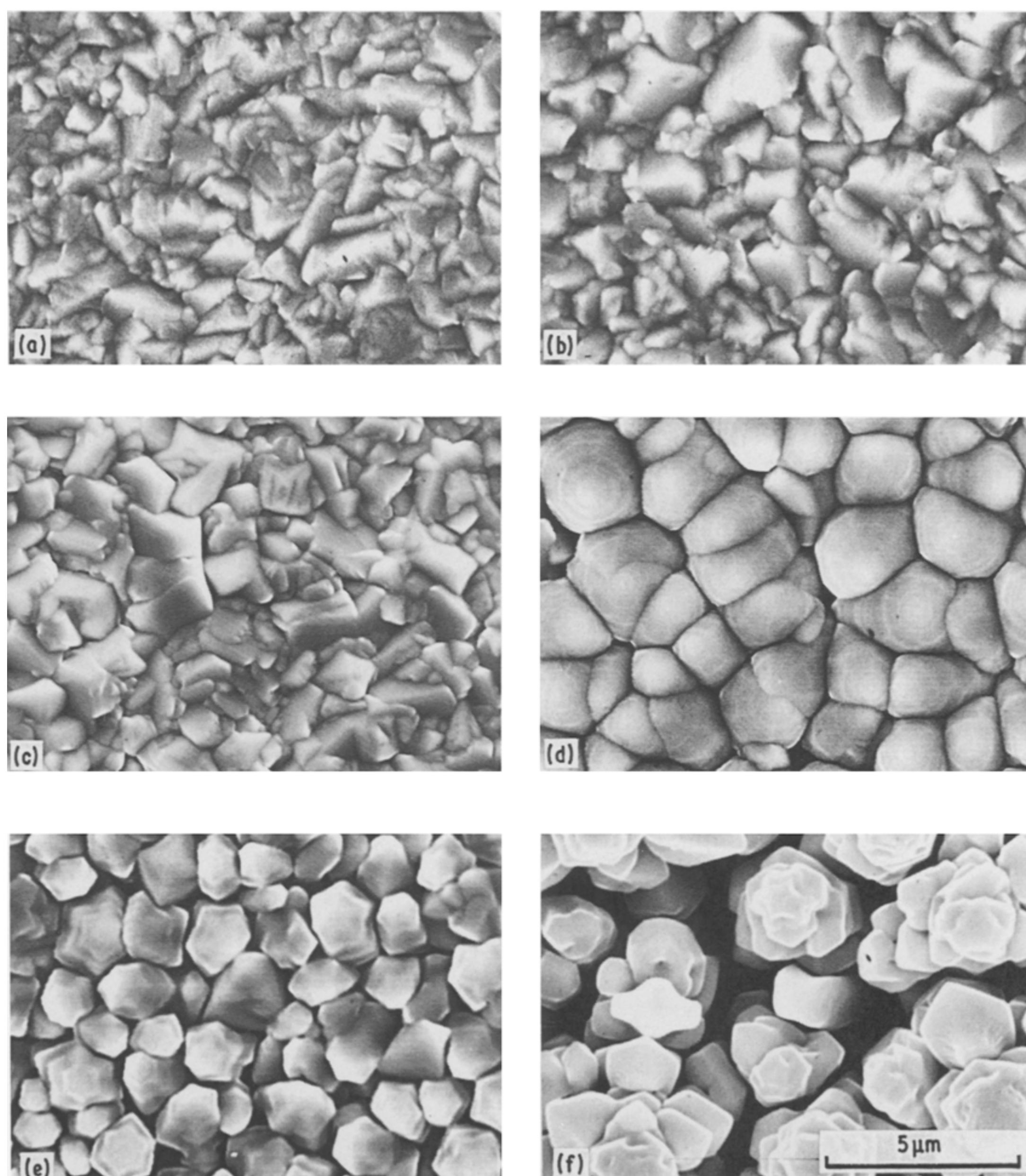

Fig. 2. Deposit morphology observed with p.c. at various N_p with N_m = 0.19. (a) 0.48; (b) 0.73; (c) 0.91; (d) 1.10; (e) 1.88; (f) 4.28.

A 20-cm^2 electrolytic copper plate forms the anode. A saturated mercury sulphate electrode is used as reference. The rotation rate in all experiments is 1000 rpm, the temperature is 25 ± 0.5° C. The electrolyte is 0.1 M $CuSO_4$ + 1 M H_2SO_4 prepared from analytical grade chemicals and doubly distilled water. The solution is deaerated by bubbling argon. Newly prepared electrolyte solutions are pre-electrolysed at a current density of 3.2 mA cm^{-2} for 15 h. This procedure was found necessary in order to obtain reproducible results, especially for the study of the morphology.

Before a deposition experiment the cathode cap is mechanically polished to a mirror finish, then cathodically prepolarized in 0.1 M H_2SO_4 for 30 s at 5 mA cm^{-2}, rinsed with water and dried in air. It is weighed on an analytical balance to 0.02 mg before and after deposition. Unless otherwise stated the charge passed is 27.2 C cm^{-2} which corresponds to a theoretical average thickness of 10 μm of copper.

Constant current pulses are supplied by a pulse generator (EGATEC, 25A–40 V). Current pulses and potential transients are monitored with a digital oscilloscope (Nicolet 206 or 3091). The deposits are observed with a Cambridge S100 or S250 scanning electron microscope.

4. Results

A first series of experiments is carried out with direct current. The measured value of the limiting current density under the experimental conditions is 60.8 ± 1.4 mA cm^{-2} and the thickness of the corresponding Nernst diffusion layer is 16.8 μm. Copper deposition is carried out at constant current density corresponding to 0.2, 0.5, 0.8, 1.2 and 2.0 times the value of the

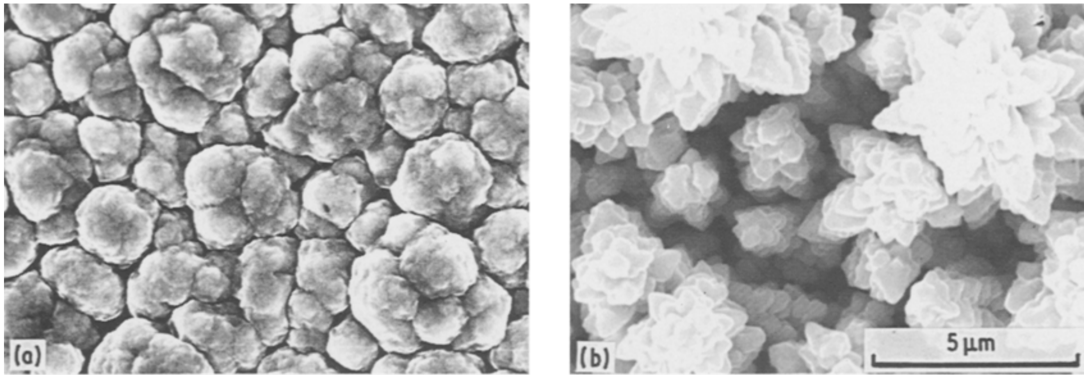

Fig. 3. Deposit morphology observed with p.c. at $N_m > 1$, $N_p > 1$: (a) $N_m = 1.2$, $N_p = 1.88$; (b) $N_m = 2$, $N_p = 4.31$.

limiting current density. The resulting surface microstructures of the deposits observed with an SEM are presented in Fig. 1. Below the limiting current the deposits are granular and compact. Above the limiting current nodular 'cauliflower-like' deposits are observed. The behaviour is consistent with the literature [20].

Pulse plating experiments are performed at an average current density corresponding to N_m values of 0.2, 0.5, 0.8, 1.2 and 2.0, respectively. N_p is varied between 0.48 and 4.31. The different experimental parameters are summarized in Table 1. For the calculation of i_{pl} a value of $D = 5.3 \times 10^{-6}\,cm^2\,s^{-1}$ is used for the diffusion coefficient of copper ions and a kinematic viscosity of $\nu = 1.03 \times 10^{-2}\,cm^2\,s^{-1}$.

Scanning electron micrographs of deposits obtained at different N_p and a constant N_m of 0.19 are shown in Fig. 2. The same general behaviour is observed at other N_m values. For $N_p = 0.5$ and $N_p = 0.7$ the observed deposits are fine-grained compact. At $N_p = 1$ and above dendritic deposits are formed.

The granular–dendritic transition is progressive rather than abrupt. The reason is that even when $N_p > 1$, a certain amount of metal is deposited under conditions not limited by mass transport, at the beginning of each pulse. Moreover, when δ_p is small, the dendrites are not very well developed (i.e. their arms are very short) and the space between them is very small (Fig. 2e), as will be shown later.

Increasing the average current density emphasizes the non-uniformity of the shapes and sizes of the dendrites (Fig. 3). However, for a given N_p there are no essential differences with Fig. 2. When N_m is large, the dendrites tend to form aggregates and they are less well defined from a crystallographic point of view.

Figure 4 summarizes the observed deposit morphologies resulting from deposition at different values of N_p and N_m. Three regions are distinguished in the N_p vs N_m parameter space; firstly region III where $N_p < N_m$ is physically unattainable, as discussed in the theoretical part. The condition $N_p > 1$ leads to dendritic deposits and, therefore, region II is to be avoided in practice. Finally, the condition $1 > N_p > N_m$ leads to compact granular deposits and, therefore, region I represents the practically useful parameter space. D.c. conditions correspond to the straight line $N_p = N_m$.

The current efficiency for copper deposition is measured as a function of N_p for constant N_m and

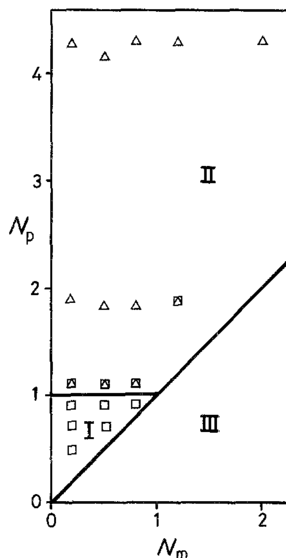

Fig. 4. Influence of mass transport parameters N_m and N_p on the type of deposits. □: Granular; △: nodular and/or dendritic; I: $N_m < N_p < 1$; II: $N_m < N_p > 1$; III: unattainable conditions.

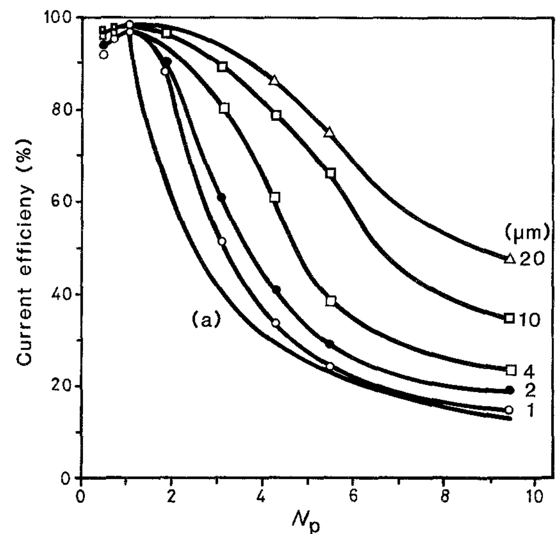

Fig. 5. Influence of N_p and of the nominal deposit thickness on the measured current efficiency. $N_m = 0.19$. Curve (a) represents the calculated current efficiency for a smooth surface.

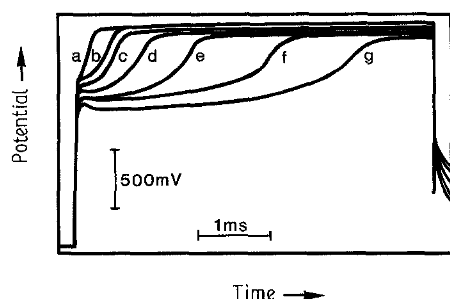

Fig. 6. Measured potential transients during pulse plating at different deposition times of (a) 5, (b) 30, (c) 60, (d) 236, (e) 452, (f) 945, (g) 2362 s. Pulse time: 5 ms.

different deposit thickness. The results obtained are shown in Fig. 5. Also indicated in the figure is a theoretical curve calculated numerically according to a procedure described elsewhere in detail [19]. The theoretical calculation shown is based on the assumption that below the pulse limiting current the current efficiency is 100%. For $i_p > i_{pl}$ hydrogen evolution takes up an increasing part of the current passed and the efficiency drops. According to this model, the efficiency depends only on N_p, whatever i_p, t_p, t_p' may be.

This is not the case experimentally, however. Variations up to 15% (for 1 μm deposits) were observed for given N_p and N_m, but various i_p, t_p, t_p'. This is more than the uncertainty of the measurements, which is smaller than 3%. These deviations from ideal behaviour might be due to formation and loss into the bulk solution of monovalent copper ion reaction intermediates [21], to a perturbation of the cathodic diffusion layer by hydrogen formation under certain conditions or to roughness effects (see below). Nevertheless, the variations are not large enough for the overall behaviour of the model to be contradicted.

The experimental data of Fig. 5 all lie above the theoretical curve and the measured current efficiencies clearly depend on the amount of deposited metal. This behaviour is due to the increase in surface roughness resulting from the formation of a dendritic deposit structure at $N_p > 1$. The effective surface area is thus always higher than the geometric surface area used for the calculation of the pulse limiting current density, i.e. the effective value of N_p is lower than the theoretical one shown on the X-axis of Fig. 5. This view

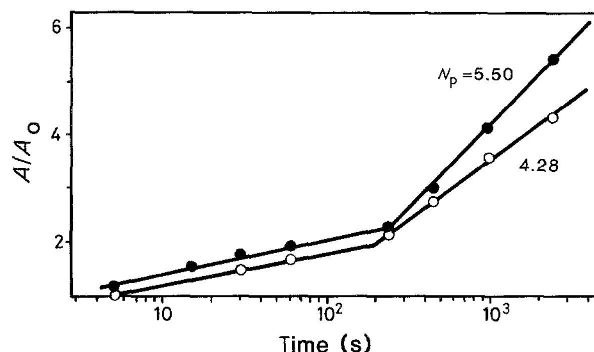

Fig. 7. Apparent surface area of the electrode (normalized to geometrical area) as a function of the deposition time.

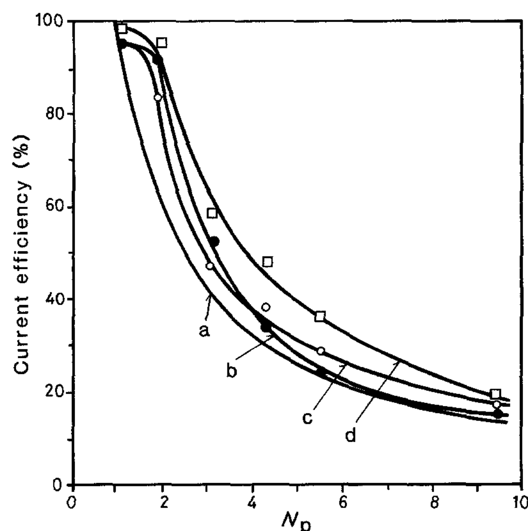

Fig. 8. Gravimetric (●) and coulometric (□, ○) measurements of the current efficiency. Nominal thickness: 64 nm (c), 1 μm (b, d). N_m = 0.19. Curve (a) represents the calculated current efficiency for a smooth surface.

is confirmed by potential measurements. In Fig. 6 measured potential transients are shown for i_p = 2.31 A cm^{-2}, t_p = 5 ms and t_p' = 999 ms (N_p = 4.28). These transients were measured in the same experiment at different deposition times as indicated. In metal deposition a potential jump occurs at the transition time τ when the concentration of the reacting species reaches zero at the electrode surface [10]. For single pulses or for repetitive pulses with $\gamma \ll 1$ the value of τ is given by the Sand equation:

$$\tau^{1/2} = \frac{kA}{I} \qquad (7)$$

where $k = nFD^{1/2}(\pi/4)^{1/2}c_b$ is a constant in our case, A is the surface area and I the applied pulse current. According to Equation 7 an increase in A for otherwise identical conditions leads to an increase in $\tau^{1/2}$. This is qualitatively consistent with the data of Fig. 6. In Fig. 7, the ratio A/A_0 where A is an apparent surface area calculated from the measured transition times using Equation 6 and A_0 is the geometrical surface area, is plotted as a function of the deposition time for two values of N_p. The data show that the value of the apparent surface area may be several times that of the geometrical one. The first straight line corresponds to the formation and growth of spherical shapes. When these reach a diameter of 0.4–0.5 μm instability develops and branches form, leading to dendritical shapes. The second line corresponds to the growth of dendrites. The apparent surface area A of Fig. 7 should not be confused with the real surface area which is probably higher and would have to be determined by other methods (e.g. BET) which are beyond the scope of the present study.

A few efficiency determinations were performed with extremely short deposition times in order to test the accuracy of the theoretical curve in Fig. 6. For this a gold RHE was used and the deposited copper was redissolved anodically at a constant current density of 12.7 A cm^{-2}. The current efficiency was then cal-

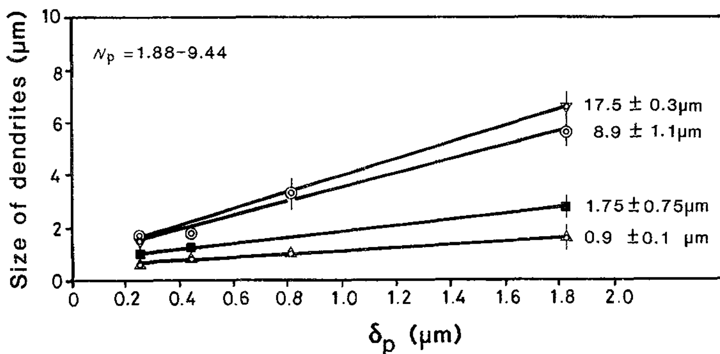

Fig. 9. Correlation between the average thickness (calculated from gravimetric data) of the pulsating diffusion layer δ_p and the mean size of the dendrites for different thicknesses of the deposit as calculated from gravimetric data, $N_m = 0.19$.

culated from the measured ratio of anodic to cathodic charge. The results are shown in Fig. 8. The measured curves lie close to the theoretical one but the measured current efficiencies are still higher, even for a theoretical average deposit thickness as small as 64 nm (deposition time: 15 s). The behaviour suggests that the deposit did not form uniformly under these conditions involving probably initial formation of islands. In such a case local spherical diffusion phenomena could lead to higher mass transport rates.

5. Discussion

The morphology of copper deposits produced by pulse plating at very high pulse current densities (up to 250 A cm^{-2}) has been studied by Ibl and Puippe [7] who concluded that compact deposits are formed well above the pulse limiting current density. The data of the present study obtained under carefully controlled conditions show that mass transport influences the morphology of copper deposits in a determining way: compact granular deposits are obtained only for pulse current densities smaller than the pulse limiting current density. If i_p exceeds i_{pl} dendritic deposits result.

Table 1. Experimental conditions for pulse plating

i_p (A cm^{-2})	t_p (ms)	t'_p (ms)	δ_p (µm)	N_p	N_m
1.16	0.1	10	0.26	0.48	0.19
0.400	3	100	1.40	0.73	
0.645	2	110	1.15	0.91	
1.16	1	100	0.82	1.10	
3.85	0.3	100	0.45	1.88	
3.66	1	317	0.82	3.12	
2.31	5	999	1.83	4.28	
3.85	3	999	1.42	5.50	
11.5	1	999	0.82	9.44	
0.335	1	10	0.78	0.73	0.5
0.548	1	17	0.80	0.91	
0.791	1	25	0.81	1.10	
1.70	1	55	0.81	1.84	
4.59	1	150	0.82	4.17	
0.341	0.2	1.2	0.34	0.90	0.8
0.438	1	8	0.77	1.10	
1.36	1	27	0.81	1.84	
4.43	1	90	0.82	4.31	
0.95	1	12	0.79	1.88	1.2
3.94	1	53	0.81	4.29	
3.04	1	24	0.81	4.31	2

The shapes and sizes of the dendrites and their microstructure depend on the applied pulse parameters and on the total amount of metal deposited. This is shown by the micrographs of Figs 1 and 2. There are strong indications that the average size of non-branching dendrites increases with increasing thickness of the pulsating diffusion layer (Fig. 9), but the reproducibility of such measurements is not always good. In practice one usually wants to avoid the formation of dendritic deposits. This is achieved by carrying out the deposition at $N_p \leq 1$ as shown in Fig. 4. The parameter space defined in this figure, therefore, provides a rational basis for the choice of deposition conditions in pulse plating.

The data of Fig. 5 demonstrate the importance of deposit morphology for current efficiency. Theoretical predictions which are based on the assumption of a flat surface are of limited usefulness if the deposition is carried out above the limiting pulse current density and involves dendrite formation. On the other hand, for small deposit thicknesses and flat deposits reasonable agreement between theory and experiment is observed. Very good agreement between theoretical and experimental data for copper deposition on a rotating disk electrode has recently been reported by Cheh [22].

Preliminary experiments performed in the present study showed that a careful choice of the experimental arrangement used for pulse plating studies is very important. For example, if relatively thick deposits are formed the use of a rotating disk electrode for the investigation of current efficiency is not advisable.

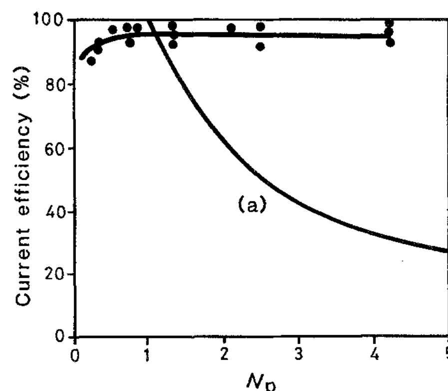

Fig. 10. Measured current efficiency on a rotating disk electrode as a function of N_p. Nominal deposit thickness 40 µm (109 C cm^{-2}). Curve (a) represents the calculated current efficiency for a smooth surface.

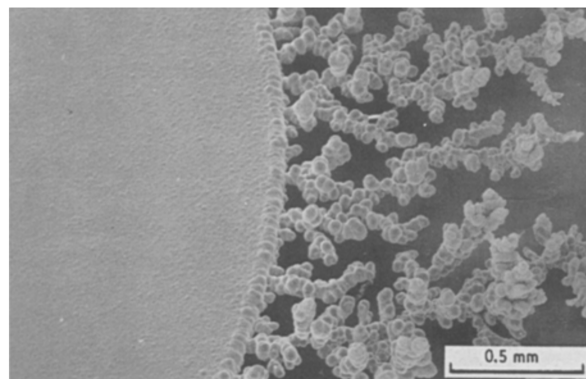

Fig. 11. Lateral growth of dendrites observed on a RDE of 8 mm diameter at $i_p = 20.3\,\mathrm{A\,cm^{-2}}$, $t_p = 0.3\,\mathrm{ms}$, $t'_p = 999\,\mathrm{ms}$. $N_p = 2.46$. The nominal deposit thickness is 40 μm.

Indeed, contrary to the rotating hemispherical electrode the primary current distribution on a disk is highly non-uniform [23]. This can lead to pronounced edge effects with dendrites growing laterally to great distances: a few mm for an average deposit thickness of 40 μm [11]. The resulting increase in surface area is thus much more pronounced than that due to dendrite growth perpendicular to the surface and measured current efficiency values are correspondingly high. The data of Fig. 10 show that on a rotating disk electrode with a nominal deposit thickness of 40 μm an almost constant current efficiency is observed at N_p values up to 4. The lateral growth of dendrites which causes this effect is illustrated in Fig. 11. The different data clearly show the need for well-defined experimental conditions in pulse plating experiments if effects due to mass transport, surface morphology and current distribution are to be identified.

6. Conclusions

In pulse plating of copper the deposit morphology depends on the prevailing mass transport conditions. The pulse parameter range leading to non-dendritic granular deposits can be advantageously presented in the N_p vs N_m plane, where the dimensionless parameters N_p and N_m characterize non-steady state and steady state mass transport, respectively. The measured current efficiency for a given set of pulse parameters is affected by the uniformity of the current distribution and by the apparent surface area, which may vary with the deposit thickness.

Acknowledgement

The authors are indebted to A. Ruffoni for providing assistance in the calculation of current efficiency.

References

[1] J. C. Puippe and F. Leaman (Editors), 'Theory and Practice of Pulse Plating', AESF (1986).
[2] AES 2nd Int. Symposium on Pulse Plating, Rosemont, AES (1981).
[3] N. M. Osero, *Plat. Surf. Finish.* **73** (1986) 20.
[4] J. C. Puippe, N. Ibl, K. Hosokawa and H. Angerer, AES Symposium on Pulse Plating, Boston (1979).
[5] E. Robert, *Oberfläche/Surface* **24**(1983) 413.
[6] B. Sutter, *Oberfläche/Surface* **25** (1984) 16.
[7] N. Ibl, J. C. Puippe and H. Angerer, *Surf. Technol.* **6** (1987) 287.
[8] J. C. Puippe, N. Ibl, H. Angerer and H. J. Schenk, *Oberfläche/Surface* **20** (1979) 77.
[9] J. C. Puippe and N. Ibl, *Plat. Surf. Finish.* **67** (1980) 68.
[10] M. Datta and D. Landolt, *Surf. Technol.* **25** (1985) 97.
[11] O. Chène, M. Datta and D. Landolt, *Oberfläche/Surface* **26** (1985) 45.
[12] D. T. Chin, *J. Electrochem. Soc.* **118** (1971) 1434.
[13] D. T. Chin, *J. Electrochem. Soc.* **119** (1972) 1049.
[14] D. T. Chin, *J. Electrochem. Soc.* **130** (1983) 1657.
[15] N. Ibl, *Surf. Technol.* **10** (1980) 81.
[16] T. R. Rosebrugh and W. L. Miller, *J. Phys. Chem.* **14** (1910) 816.
[17] A. M. Presco and H. Y. Cheh, *J. Electrochem. Soc.* **131** (1984) 2259.
[18] H. Y. Cheh, *J. Electrochem. Soc.* **118** (1971) 551.
[19] A. Ruffoni, Thèse EPFL No. 683 (1987).
[20] N. Ibl, in 'Advances in Electrochem. and Electrochemical Engineering', Vol. 2 (edited by C. W. Tobias), Interscience (1966) pp. 48–143.
[21] C. C. Wan, H. Y. Cheh and H. B. Linford, *J. Appl. Electrochem.* **9** (1979) 29.
[22] H. Y. Cheh and T. Cheng, in 'Electrodeposition Technology, Theory and Practice' (edited by L. T. Romankiw and D. R. Turner), ECS (1987) p. 555.
[23] J. Newman, *J. Electrochem. Soc.* **113** (1966) 1235.